

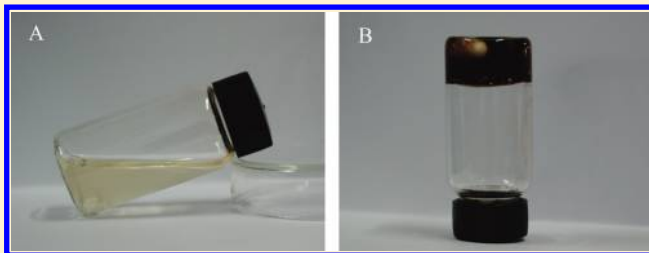
Novel Redox Hydrogel by in Situ Gelation of Chitosan as a Result of Template Oxidative Polymerization of Hydroquinone

Jian He, Aijuan Zhang, Yongjun Zhang,* and Ying Guan*

Key Laboratory of Functional Polymer Materials, Institute of Polymer Chemistry, College of Chemistry, Nankai University, Tianjin 300071, China

S Supporting Information

ABSTRACT: A new redox hydrogel using poly(hydroquinone) (PHQ) as polymeric redox couple and chitosan as matrix was synthesized by simple exposing an acidic chitosan/hydroquinone (HQ) solution to the air. PHQ was synthesized in situ by oxidative polymerization of HQ using oxygen as an oxidant. The presence of chitosan increases the reaction rate significantly, suggesting chitosan works as a template for the polymerization of HQ. The reaction rate increases linearly with chitosan concentration when molar ratio of chitosan/HQ is less than 0.96 but keeps constant beyond that point. These results suggest a pick-up mechanism for the template polymerization of HQ. The polymerization of HQ further results in the gelation of the aqueous solution, as physical cross-links forms between PHQ and chitosan. The gelation time decreases with increasing chitosan and HQ concentration and also increasing temperature. The resultant hydrogel are redox-active. Cyclic voltammogram of the hydrogel presents two oxidation peaks at 0.62 and 1.23 V and two reduction peaks at -0.79 and -1.66 V (vs Ag/AgCl). The in situ-formed redox hydrogel may find applications in biomedical areas.



INTRODUCTION

Redox hydrogels are hydrogels containing redox couples that are either trapped in or bound to the cross-linked polymer network.¹ The hydrated hydrogel matrix allows for the diffusion of water-soluble chemicals and biochemicals, while the redox couples conduct electrons by self-exchange of electrons or holes between rapidly reduced and rapidly oxidized redox functions. These materials have wide applications in amperometric biosensors,^{2,3} biofuel cells,⁴ and bioelectrochemomechanical energy conversion.⁵

Common redox couples include quinoid functions,⁶ ferrocene⁷ and $\text{Os}^{2+/3+}$,⁸ which are usually tethered on the polymer network through covalent or coordinative bonds. Polymeric redox couples, such as polyaniline² and polypyrrole,⁹ have also been employed by trapped in a hydrogel matrix. Compared with polyaniline and polypyrrole, which have been extensively studied in the literature, poly(hydroquinone) (PHQ), which is also redox-active, received much less attention, although it is very attractive as redox polymer because it can undergo direct two-electron oxidation and reduction.¹⁰

PHQ can be readily synthesized by oxidative polymerization of hydroquinone (HQ) or *p*-benzoquinone in alkali solutions.^{11,12} By electrooxidative polymerization of HQ, PHQ films can be deposited on electrodes.¹³ To obtain products with well-defined structures, sophisticated biochemical process¹⁰ and organometallic polycondensation process¹⁴ were developed. The electron transfer between electrode and glucose oxidase can be effectively mediated by PHQ, therefore it can be used as a mediator for amperometric glucose sensors.¹⁵

In this work a new redox hydrogel was synthesized using PHQ as polymeric redox couples and chitosan as hydrogel matrix. Chitosan is a polysaccharide composed of β -(1-4)-linked *N*-acetyl-D-glucosamine and D-glucosamine. Because of its biocompatibility and biodegradability, this pseudonatural polymer has found numerous biomedical applications including gene delivery,¹⁶⁻¹⁸ tissue engineering,¹⁹ drug delivery²⁰ and wound dressings.^{21,22} The redox polymer, PHQ, is synthesized by oxidative polymerization of HQ in *acidic* solutions using chitosan as template, instead of in *alkali* solutions. To the best of our knowledge, this is the first report of the template oxidative polymerization of HQ. The resultant PHQ forms hydrogen bonds with chitosan and physically gels the solution. The *in situ*-formed hydrogel is redox-active and may find applications in biomedical areas.

EXPERIMENTAL SECTION

Materials. Chitosan with viscosity of 50.0–800.0 mPa·s and D.D (degree of deacetylation) $\geq 90\%$ was purchased from Sinopharm Chemical Reagent Co., Ltd. The M_w was measured to be $\sim 5.47 \times 10^5$ by GPC (Figure 1S, Supporting Information). D-glucosamine hydrochloride, hydroquinone (HQ), ethylenediaminetetraacetic acid (EDTA), acetic acid (HAc), urea and other chemicals are of analytical grade.

Received: March 19, 2010

Revised: February 9, 2011

Published: March 04, 2011

Purification of Chitosan. The chitosan sample was purified according to Allan and Peyron.²³ 0.1 g of chitosan was dissolved in 50 mL of 0.1 M HAc. It was precipitated with methanolic ammonia (70% methanol and 30% aqueous $\text{NH}_3 \cdot \text{H}_2\text{O}$). The solid obtained was washed 4 times with deionized water and 3 times with acetone, and dried at 35 °C under reduced pressure.

Oxidative Polymerization of HQ Using Chitosan as Template. As a typical experiment, chitosan (0.5 g) was dissolved in 50 mL of 0.1 M HAc by stirring overnight. The solution was transferred to a three-necked flask equipped with a condenser and heated to 60 °C. A 0.5 g sample of HQ was added, and the mixture was stirred at 60 °C until the solution gelled.

Separation of PHQ from Chitosan/PHQ Hydrogel. To the chitosan/PHQ hydrogel obtained in previous step were added 10 mL of 0.40 M NaNO_2 and 2 mL of 0.05 M HCl. The mixture was stirred at 60 °C overnight. With the depolymerization of chitosan, the hydrogel disappeared and a dark precipitate was obtained. After filtered and washed with water, the precipitate was dried in a vacuum oven at 70 °C.

In a second method, HCl and H_2O_2 were added to the chitosan/PHQ hydrogel to degrade chitosan. Final concentration of HCl and H_2O_2 was 0.45 and 5 wt %, respectively. The mixture was stirred at 90 °C for 2 h. Solid product was collected on a filter, washed with water and dried in a vacuum oven at 80 °C.

Synthesis of PHQ by Oxidative Polymerization of HQ in Alkali Solution. PHQ was also synthesized by oxidative polymerization of HQ in alkali solution according to ref 11 as follows: 5.5 g of HQ was dissolved in 60 mL of water containing 2.8 g of KOH. Air, which was purified by washing with 1 M NaOH, was bubbled into the solution. A black viscous mixture was obtained after 22 h of air bubbling. A 6 mL aliquot of concentrated HCl was added, and a black-brown precipitate was obtained. The solid was collected by filtration, washed repeatedly with water, and dried for 1 day in air and then in vacuum oven at 100 °C.

Characterization. UV–vis absorption spectra were measured on a TU 1810PC UV–vis spectrophotometer (Purkinje General, China). Fourier transform infrared (FTIR) spectra were measured on a Bio-Rad FTS-6000 spectrometer. ^1H NMR spectra were recorded on a Varian UNITY-plus 400 NMR spectrometer using $\text{DMSO}-d_6$ as solvent. GPC was carried out on Waters with 2414 refractive index detector and Styragel HT3, HT4 and HT5 Columns at 50 °C using DMF eluent at a flow rate of 1.0 mL/min.

Rheological characterization of the reaction mixture was performed on an AR2000ex rheometer (TA Instruments). Parallel plate geometry with a diameter of 40 mm was used. The sample gap was set to be 1.0 mm. The temperature was controlled by a Peltier system in the bottom plate connected with a water bath. Electrochemical characterization of the hydrogel was performed on a LK98B II electrochemical analysis system (Lanlike, China). The hydrogel was smeared on a glassy carbon (GC) electrode and dried in air. Impurities were removed by repeated soaking in water. Cyclic voltammetry (CV) measurements were performed in 0.05 mol/L phosphate buffer (pH = 7.3), using platinum and Ag/AgCl (saturated KCl) as the counter electrode and the reference electrode, respectively. The solutions were deoxygenated by bubbling nitrogen gas.

RESULTS AND DISCUSSION

Oxidative Polymerization of HQ using Chitosan as Template. We accidentally observed that when exposed to the air, the color of an acidic solution of chitosan and HQ gradually turns from light yellow to wine. At the same time, the solution gets more and more viscous. Finally it can not flow any longer and a dark brown hydrogel forms.

We hypothesize that HQ may polymerize and the resultant PHQ polymer forms hydrogen bonds with chitosan and gels the aqueous solution. The proposed reaction and the interaction

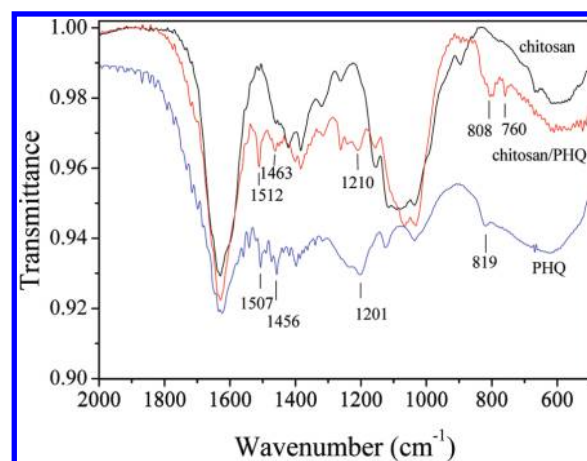
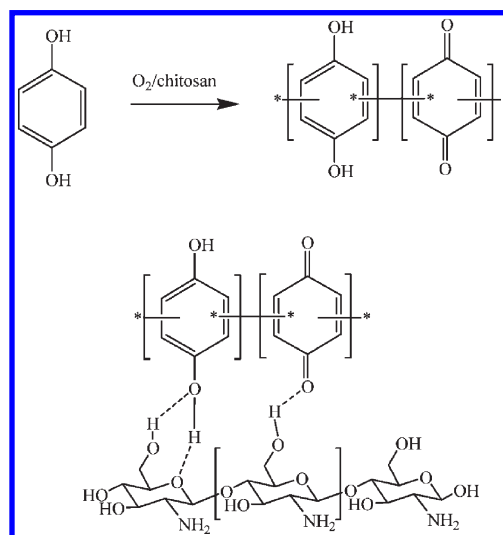


Figure 1. FTIR spectra of chitosan, chitosan/PHQ hydrogel prepared in this work, and PHQ synthesized by oxidative polymerization in alkali solution.

Scheme 1. Oxidative Polymerization of HQ Using Chitosan as Template and the Hydrogen Bonding between PHQ and Chitosan^a



^a For chitosan, only the D-glucosamine units were depicted. The PHQ structure was depicted according to ref 11.

between chitosan and PHQ were schematically depicted in Scheme 1. FTIR spectra of the dried hydrogel provide evidence for the formation of PHQ. Figure 1 shows the FTIR spectra of the dried hydrogel, chitosan and PHQ synthesized by oxidative polymerization of HQ in alkali solution. Compared with the IR spectra of chitosan, several new peaks appear in the spectra of the hydrogel. Almost all these peaks can also be found in the spectra of PHQ, suggesting that PHQ involved in the hydrogel. In particular, the new peaks at 1512 and 1463 cm^{-1} can be assigned to the vibrations of aromatic rings and $\text{C}=\text{C}$ bonds in the backbone of PHQ. The peak at 1210 cm^{-1} can be assigned to the phenolic OH groups. Peaks at 808 and 760 cm^{-1} can be assigned to the out-of-plane vibrations of the $\text{C}-\text{H}$ bonds of the aromatic rings.^{24–26}

UV–vis spectra of the product also confirm the formation of PHQ. To separate PHQ from the hydrogel, the raw product was

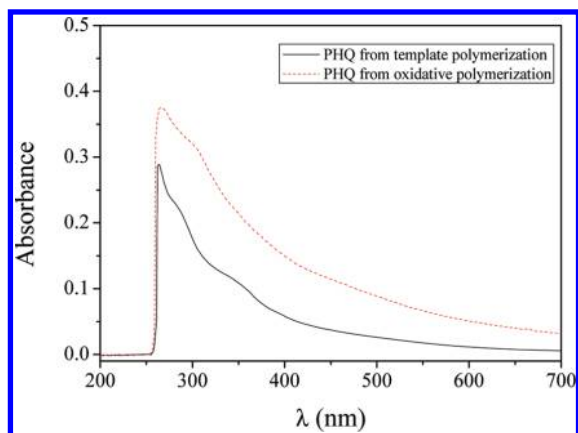


Figure 2. UV-vis spectra of PHQ obtained by oxidative polymerization of HQ in alkali solution and that synthesized in this work. The solvent is DMSO.

first treated with nitrous acid to depolymerize chitosan.²³ Some dark solid was obtained, which are partially soluble in DMSO. The UV-vis spectra of the DMSO solution are shown in Figure 2, from which a peak at 264 nm and two shoulders at 285 and 350 nm were found. For comparison, the spectra of PHQ synthesized by oxidative polymerization of HQ in alkali solution were also included. One can find that the shape of the two spectra is similar. Similar absorption spectra of PHQ synthesized by oxidative polymerization of HQ or benzoquinone in alkali solutions have been reported.¹¹

“Pure” PHQ was also obtained by degradation of chitosan with H_2O_2 .²⁷ The product obtained using this method has a higher solubility in DMSO and DMF, which allows for NMR and GPC characterization. ^1H NMR of the product (in $\text{DMSO}-d_6$) show signals from 6.5 to 7.8 ppm, which is assigned to aromatic or quinone protons, and a broad peak at 10.3 ppm, which is assigned to phenolic hydroxyl protons (Figure 2S, Supporting Information). The NMR spectrum of the product is similar to that synthesized by Dordick et al.¹⁰ On the basis of these observations, we speculate that the PHQ polymer synthesized here has a structure as shown in Scheme 1, similar to PHQ synthesized by oxidative polymerization in alkali solution.¹¹ The M_w of the polymer was measured to be 8800 by GPC (Figure 3S, Supporting Information), which is close to that synthesized by polycondensation.¹⁴

PHQ is an attractive redox polymer which can be used in electrical conductors, batteries, electrode coatings for sensors, catalysts for electrochemical reactions, antioxidants, and corrosion or degradation reaction inhibitors.¹⁰ As mentioned before, there are several synthesis methods reported in the literature, including oxidative polymerization of HQ or benzoquinone in alkali solutions,^{11,24–26} electrochemical polymerization of HQ,¹³ enzymatic method¹⁰ and polycondensation method.¹⁴ It is well-known that HQ polymerizes in alkali solutions; however, it is relatively stable in acidic solutions.

To study the reaction, the initial stage of this reaction was monitored by UV-vis. As shown in Figure 3, the absorption of the reaction mixture in the visible range is negligible at the beginning, but increases with time. Five hours later, a broad peak appears at 400 nm which continues to move to longer wavelength with time. The evolution of absorption peak in the visible region indicates the generation of large conjugated structures. The inset of Figure 3 plots absorbance at 470 nm versus time. A good linear

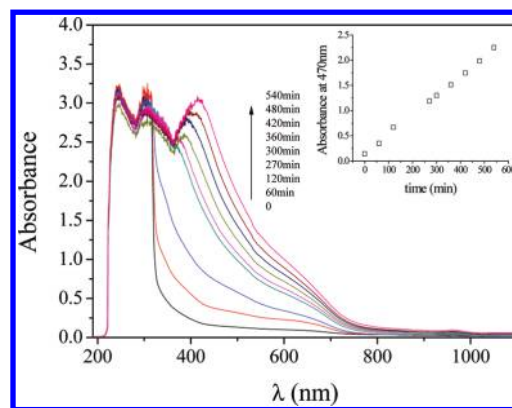


Figure 3. UV-vis spectra of HQ/chitosan mixture in 0.1 M HAc. The spectra were measured at 0, 60, 120, 270, 300, 360, 420, 480, and 540 min, respectively. $[\text{HQ}] = 3.0 \text{ wt } \%$. $[\text{chitosan}] = 1.0 \text{ wt } \%$. $T = 60^\circ\text{C}$. Inset: plot of absorbance at 470 nm versus time.

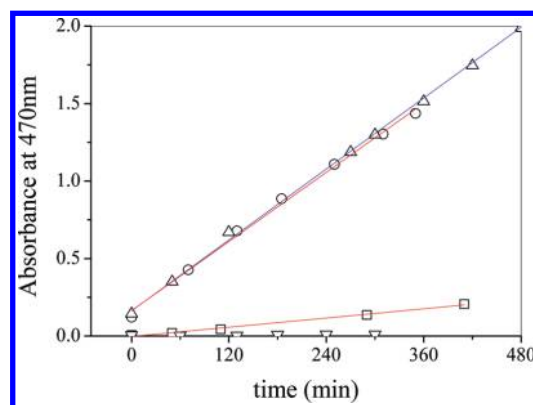


Figure 4. Plots of absorbance at 470 nm of various systems versus time: (O) 1.5 g of HQ and 0.5 g of chitosan in 50 mL of 0.1 M HAc; (V) 1.5 g of HQ and 0.5 g of chitosan in 50 mL of 0.1 M HAc purged with nitrogen; (□) 1.5 g of HQ in 50 mL of 0.1 M HAc; (Δ) 1.5 g of HQ, 0.5 g of chitosan and 0.064 g of EDTA in 50 mL of 0.1 M HAc. Temperature: 60°C .

relationship was found, suggesting that the apparent reaction rate could be conveniently represented by the absorption increase of the mixture, i.e., the slope of the absorption–time plot. To study the effects of various experimental variables, a series of experiments were conducted. The results were summarized in Figures 4 and 5. All the experiments were carried out at 60°C and in 0.1 M HAc. Good linear relationship between the absorption at 470 nm and time was found in all cases.

From Figure 4, the apparent reaction rate was measured to be 0.00372 (i.e., the slope of the absorption–time plot, similarly hereinafter) when $[\text{HQ}] = 3.0 \text{ wt } \%$ and $[\text{chitosan}] = 1.0 \text{ wt } \%$. To study the effect of oxygen, in another experiment oxygen was removed by purging with nitrogen. In this case the change in absorption at 470 nm is negligible and the apparent reaction rate was measured to be zero. (Figure 4) This result reveals that the reaction can not proceed in the absence of oxygen. Linear increase in absorption was also observed in the absence of chitosan but with a much slow rate. The apparent reaction rate was measured to be only 0.00050. The reaction rate in the presence of chitosan is more than 7 times of that in the absence of chitosan, clearly indicating the acceleration of the reaction by chitosan. It was reported that some heavy metal ions, which may

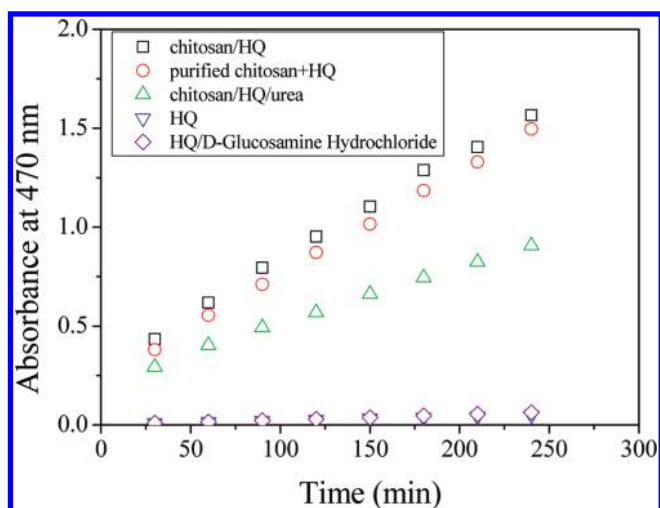


Figure 5. Plots of absorbance at 470 nm of various systems versus time: (\square) 0.8 g of chitosan (untreated) and 1.0 g of HQ in 50 mL of 0.1 M HAc; (\circ) 0.8 g of Chitosan (purified) and 1.0 g of HQ in 50 mL of 0.1 M HAc; (Δ) 0.8 g of chitosan (untreated), 1.0 g of HQ, and 24 g urea in 50 mL of 0.1 M HAc; (∇) 1.0 g of HQ in 50 mL of 0.1 M HAc; (\diamond) 1.071 g of D-glucosamine hydrochloride and 1.0 g of HQ in 50 mL 0.1 M HAc. Temperature: 60 °C.

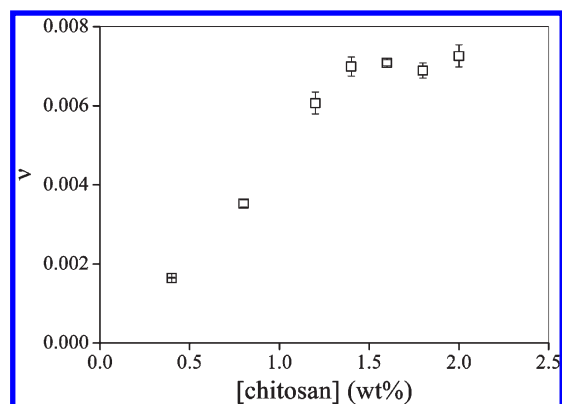


Figure 6. Reaction rate ν as a function of the concentration of chitosan. $[HQ] = 1.0$ wt %. $T = 60$ °C. In 0.1 M HAc.

exist in the chitosan samples, can catalyze the oxidation of HQ.²⁸ To rule out this possibility, EDTA, as chelator of heavy metal ions, was added. The reaction still proceeds with a reaction rate almost identical to that in the absence of EDTA. The result indicates it is chitosan rather than heavy metal ions which acts as catalyst in the reaction. To further rule out the possibility that any other impurity could be responsible for the HQ polymerization, the chitosan sample was purified by dissolution in HAc solution and precipitated with methanolic ammonia.²³ As shown in Figure 5, the reaction rate in the presence of the purified chitosan and the untreated one is almost the same. (Figure 5) On the basis of these observations, we conclude that the polymerization of HQ takes place using oxygen as an oxidant and chitosan as a template. It is noteworthy that the reaction can not be accelerated by D-glucosamine, the “monomer” of chitosan. (Figure 5)

The apparent reaction rates at various $[chitosan]$ while keeping a constant $[HQ]$ of 1.0 wt % were measured and plotted in Figure 6. The reaction rate first increases linearly with increasing $[chitosan]$, but keeps constant when $[chitosan]$ is higher than 1.4

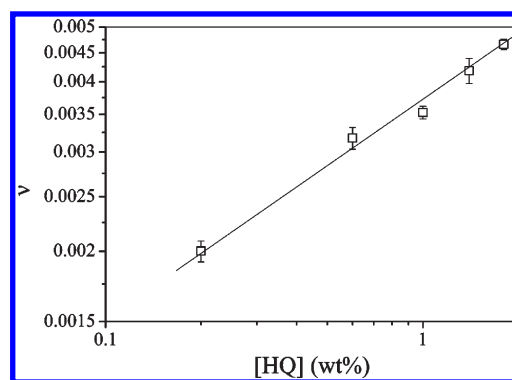


Figure 7. Reaction rate ν as a function of the concentration of HQ. $[chitosan] = 0.8$ wt %. $T = 60$ °C. In 0.1 M HAc.

wt %, where the molar ratio of chitosan repeat unit to HQ is ~ 0.96 .

Usually template polymerization proceeds according to two different mechanisms, i.e., type I or “zip” mechanism and type II or “pick up” mechanism, depending on the strength of the interaction between the monomer and the template.²⁹ The polymerization follows the “zip” mechanism when the monomers are connected with the template by strong forces. On the contrary, when the interactions between the monomers and the template are weak, the monomer at the beginning of the reaction is “free” and polymerization starts outside the template. When the growing chains reach a critical length, they bind with the template and propagate along the template by addition of monomer molecules from the surrounding solution. The two mechanisms can be distinguished by the reaction kinetics. For type I template polymerization, the reaction rate increases with increasing template concentration until the molar ratio of template to monomer reaches 1. Beyond this point, the reaction rate **decreases** with increasing template concentration. For type II template polymerization, the reaction rate also first increases with increasing template concentration, but **levels off** when the molar ratio of template to monomer reaches a critical value. The kinetics of the chitosan-templated oxidative polymerization of HQ suggests this reaction should proceed according to the type II mechanism. From this mechanism, HQ monomers are not preorganized on the chitosan template. The oligomers form first in the solution, then bind with the template and continue to propagate along the template. Considering that relatively weak hydrogen-bonding is the only interaction between chitosan and HQ, it is reasonable that the template polymerization follows the type II mechanism. Hydrogen-bonding as the main interaction between HQ and chitosan was confirmed by the reduced reaction rate in the presence of urea, a hydrogen-bond-breaking reagent (Figure 5).³⁰

The reaction rates at various $[HQ]$ while keeping a constant $[chitosan]$ of 0.8 wt % were also measured. As shown in Figure 7, the reaction rate increases with increasing $[HQ]$. A linear relationship was found from the double-log plot. The order of reaction for HQ was calculated to be 0.375 from the slope.

The apparent reaction rate as a function of temperature was plotted in Figure 8A. The data were measured at $[HQ] = 1.0$ wt % and $[chitosan] = 1.0$ wt % and in 0.1 M HAc. As can be seen, the reaction rate increases exponentially with temperature. The plot of $\ln \nu$ vs $1/RT$ is shown in Figure 8B. The apparent activation energy of the reaction was calculated to be 70.0 kJ/mol according to Arrhenius equation.

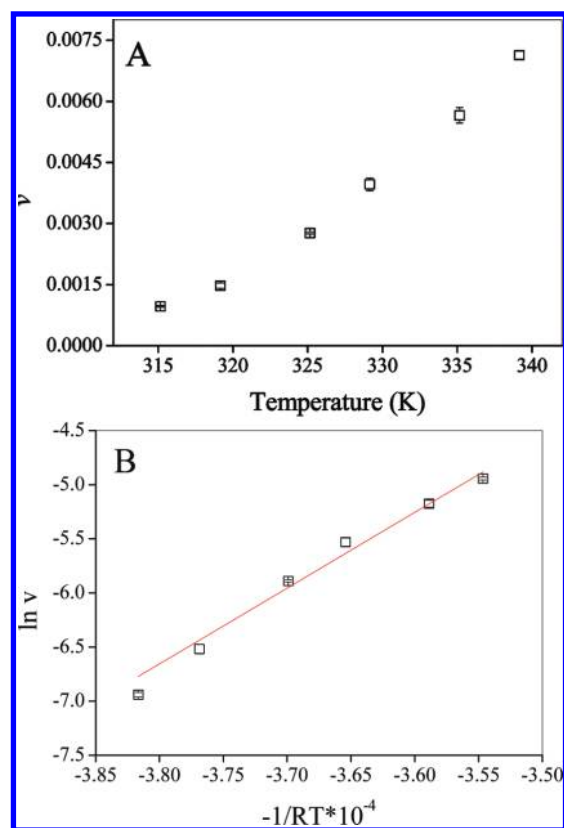


Figure 8. (A) Reaction rate ν as a function of temperature. [Chitosan] = 1.0 wt %. [HQ] = 1.0 wt %. In 0.1 M HAc. (B) Plot of $\ln \nu$ as a function of $-1/RT$.

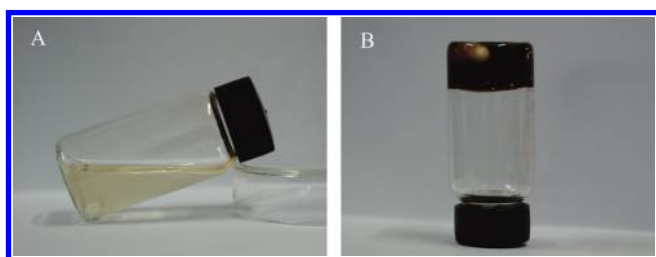


Figure 9. Photographs of chitosan/HQ solution in 0.1 M HAc before (A) and after gelation (B). [chitosan] = 1.6 wt %. [HQ] = 1.0 wt %. The solution was exposed to air and stirred at room temperature. Reaction time is 0 and 84 h for A and B, respectively.

In situ Gelation of Chitosan Solution. As we mentioned above, the template polymerization of HQ finally results in the gelation of the aqueous solution. A picture of the *in situ*-formed hydrogel is shown in Figure 9. The gelation process was studied by tracing the variation of the rheological properties. A representative result of dynamic strain sweep of the system before gelation is shown in Figure 10A. G'' dominates G' over the entire strain range we studied, indicating a liquid nature. Parts B and C of Figure 10 show the representative results of dynamic strain sweep and frequency sweep of the system after gelation. In both cases G' dominates G'' , clearly indicating the material behaves more like a solid. The results suggest the formation of a cross-linked network. From Figure 10B, both G' and G'' are independent of strain amplitude when strain is below 150%. Beyond this point, both G' and G'' increase with increasing strain, however,

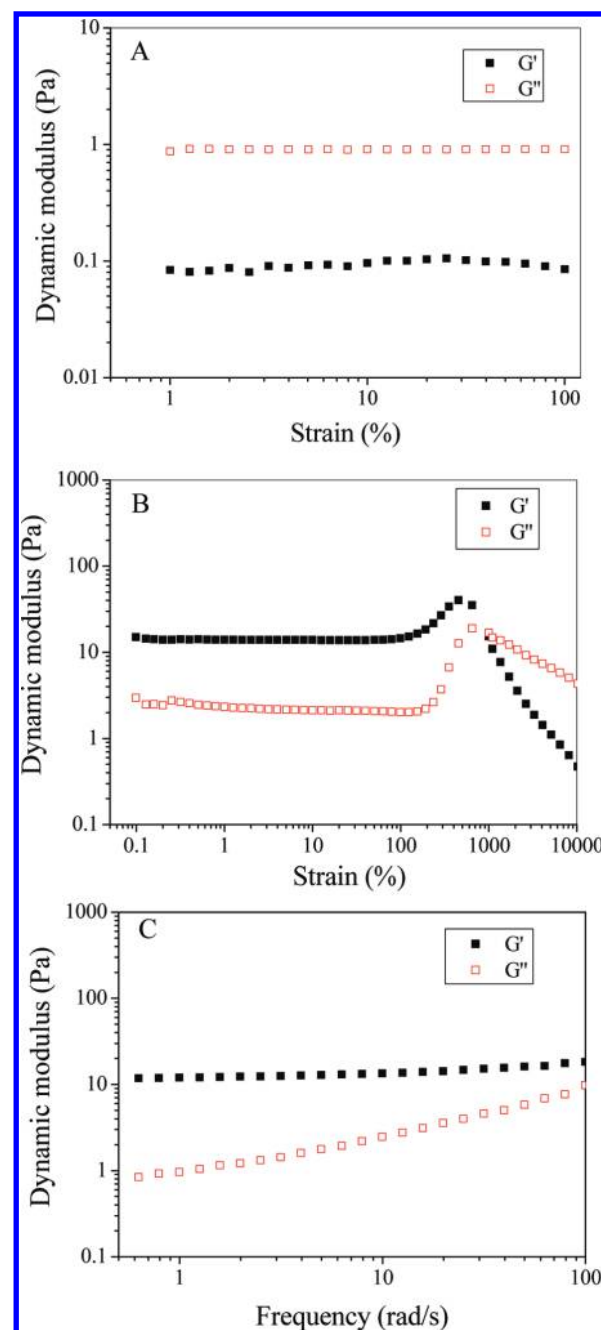


Figure 10. (A) Storage and loss moduli (G' and G'') of a chitosan/HQ solution before gelation in a dynamic strain sweep with a frequency of 0.6283 rad/s at 25 °C. The solution was prepared by dissolving 0.9 g of chitosan and 0.5 g of HQ in 50 mL 0.1 M HAc. Before rheological measurement, the solution has been kept at 60 °C for 45 min. (B, C) G' and G'' of the *in situ* formed hydrogel in a dynamic strain sweep with a frequency of 0.6283 rad/s (B) and a frequency sweep with a strain of 1% (C) at 25 °C. The gel was prepared by keeping the chitosan/HQ solution at 60 °C for 8 h. [chitosan] = 1.6 wt %. [HQ] = 1.0 wt %.

they decreases when strain increases further. A crossover was observed at a strain of 1000%, indicating the breakage of the physical network by shear force. The upturn of G' following the linear viscoelastic area is an unusual phenomenon. Previously Bhowmick et al observed a similar phenomenon from fluoroe-lastomer/clay nanocomposites, which was explained by increased crystallinity under shear.³¹ The increasing G' of

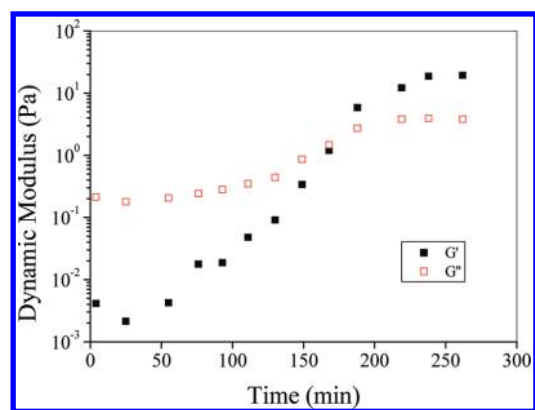


Figure 11. Evolution of G' and G'' of the chitosan/HQ solution with time. [chitosan] = 1.5 wt %. [HQ] = 1.0 wt %. Strain sweeps were carried out with a frequency of 0.6283 rad/s at 25 °C.

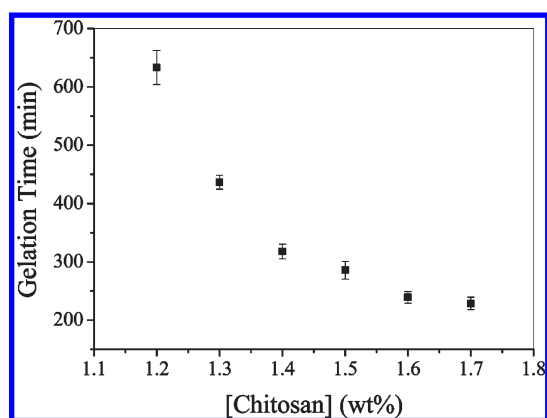


Figure 12. Gelation time as a function of the concentration of chitosan. [HQ] = 1.0 wt %. $T = 60$ °C. In 0.1 mol/L HAc.

chitosan/PHQ hydrogel may be explained in a similar way, i.e., microcrystalline of chitosan may form under shear and act as additional cross-links. From Figure 10C, both G' and G'' increase slightly with increasing frequency. Both moduli are relatively frequency-independent, which are typical of gel networks possessing long-lived cross-links.³² The relatively large loss modulus ($\tan \delta \sim 0.1$) of the hydrogel may imply the presence of a sizable sol fraction, however, network imperfections can also result in large loss modulus.

Online rheological measurement has been widely used to study the gelation process of various systems. However, the gelation of the present system can not be traced online because the fixtures will block oxygen which is used as oxidant in the oxidative polymerization of HQ, therefore it was traced off-line by taking out an aliquot of the reaction mixture at pre-determined time intervals and measuring the rheological properties immediately. G' and G'' were then plotted as a function of reaction time. As shown in Figure 11, G'' is larger than G' at the beginning. Both of them increase with time, but G' increases with a faster rate and finally exceeds G'' . The time where G' and G'' crossover can be defined as the gelation time of the system. Using this method, the effects of different experimental variables, such as [chitosan], [HQ], and temperature, on gelation time were studied. The results are shown in Figures 12–14, respectively.

Figure 12 shows that the gelation time decreases with increasing chitosan concentration. It takes ~ 630 min to gelate when

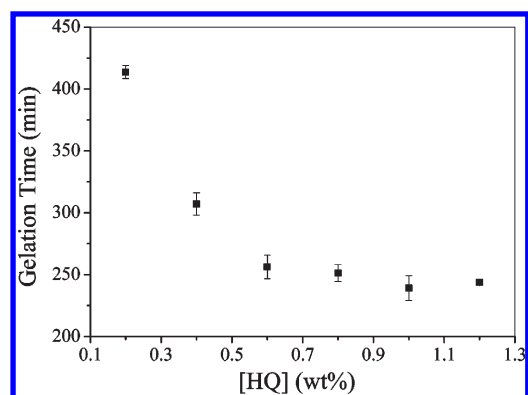


Figure 13. Gelation time as a function of the concentration of HQ. [chitosan] = 1.6%, $T = 60$ °C, in 0.1 mol/L HAc.

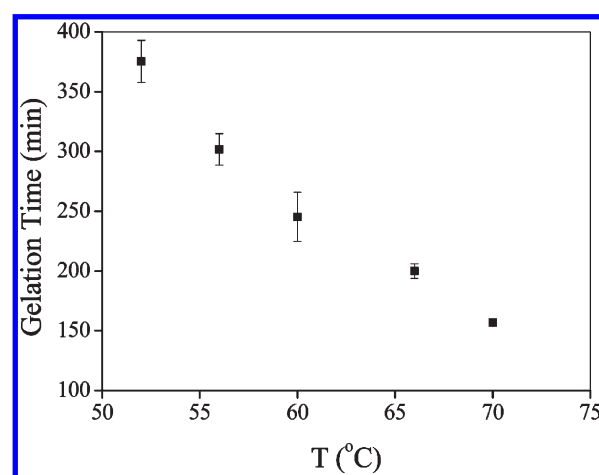


Figure 14. Gelation time as a function of the temperature. [HQ] = 1.0%, [chitosan] = 1.6%, in 0.1 mol/L HAc.

[chitosan] = 1.2 wt %, but only ~ 230 min when [chitosan] = 1.7 wt %. The gelation of the chitosan/HQ mixture can be regarded as the formation of a chitosan network by cross-linking the individual chitosan chains with PHQ, which is the product of the *in situ* oxidative polymerization of HQ. Therefore, the faster the polymerization takes place, the shorter the gelation time will be. From Figure 6, however, the reaction rate of oxidative polymerization keeps almost constant at this range of chitosan concentration. Therefore, the decrease in gelation time should be attributed to the increased possibility for the formation of cross-links at high chitosan concentration. The effect of [HQ] on gelation time is shown in Figure 13. As expected, the gelation time decreases from ~ 440 min to ~ 180 min when [HQ] increases from 0.2 wt % to 0.6 wt %. As [HQ] increases, the rate of its polymerization increases accordingly (Figure 7), therefore the physical network forms at a higher speed. However when further increasing [HQ] from 0.6 wt % to 1.2 wt %, only a slight decrease in gelation time was observed. The main reason may be the increase in polymerization rate slows down at this [HQ] range (Figure 7). The effect of temperature on gelation time is shown in Figure 14. As temperature rising, the oxidative polymerization of HQ proceeds at a higher rate. Therefore, it takes less time for the reaction mixture to gelate.

Electrochemical Properties. To study the electrochemical properties of the hydrogel, it was cast on GC electrode, and the

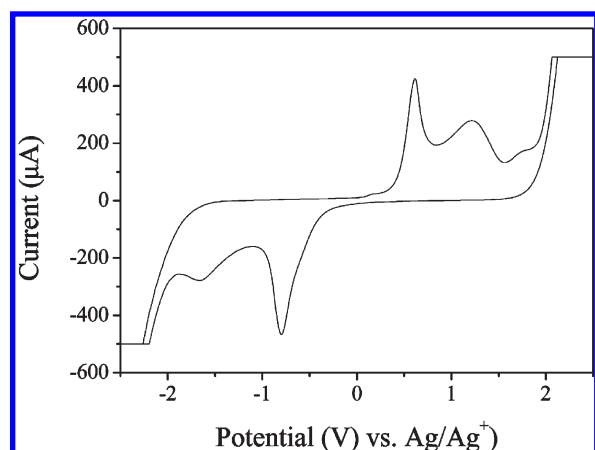
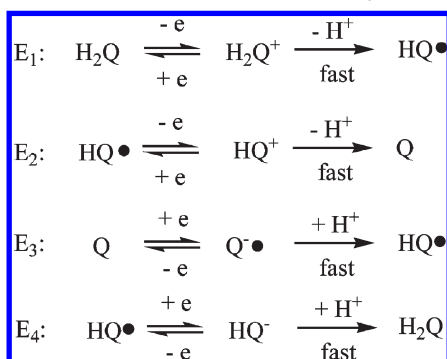


Figure 15. Cyclic voltammogram of the chitosan/PHQ hydrogel in 0.05 mol/L phosphate buffer (pH = 7.3). The sweeping velocity is 0.1 V/s. Reference electrode: Ag/AgCl. Working electrode: GC.

cyclic voltammograms were measured in 0.05 mol/L phosphate buffer (pH = 7.3). As shown in Figure 15, the hydrogel shows two oxidation peaks at 0.62 and 1.23 V and two reduction peaks at -0.79 and -1.66 V (vs Ag/AgCl). The redox potential of hydrogel was calculated from the midpoint of the first anodic and first cathodic peak potentials to be 0.085 V, which is nearly the same as the reported redox potential of the benzoquinone/HQ redox pair at pH 7 (0.09 V vs Ag/AgCl).⁶ The CV chart of the chitosan/PHQ hydrogel is similar to that of PHQ synthesized by organometallic polycondensation of dihaloaromatic compounds.¹⁴ Similarly, the CV data can be explained by the following electrochemical reactions including H^+ transfer, which was proposed based on the electrochemical behavior of HQ:¹⁴



On the CV chart of chitosan/PHQ hydrogel, the two oxidation peaks and two reduction peaks are well separated. In contrast, these peaks are not clearly separated on CV of PHQ synthesized by organometallic polycondensation.¹⁴ In addition, the CV chart of chitosan/PHQ hydrogel is symmetric in shape, indicating that the electrochemical reactions involved are reversible. Repeated scanning does not change the CV curve (data not shown), indicating that PHQ in the hydrogel is stable. Previously Yamamoto et al. showed that the electrochemical behavior of PHQ (synthesized by organometallic polycondensation) strongly depends on whether the polymer is in solution or in the solid state (film). When dissolved in DMF, repeated scanning gave almost the same CV curve, however, CV curve of a film strongly depended on the repeating number of scanning, because the film provides hydrophobic circumstances for the quinone

unit.¹⁴ On the opposite, for chitosan/PHQ hydrogel studied here, as PHQ is dispersed in the chitosan matrix which provides a hydrophilic environment for the quinone unit, the hydrogel behaviors like a real solution.

In conclusion, we synthesized a new redox hydrogel using PHQ as polymeric redox couple and chitosan as matrix. PHQ was synthesized *in situ* by oxidative polymerization of HQ using oxygen as an oxidant and chitosan as a template. The resultant PHQ in turn physically cross-links chitosan chains and gels the aqueous solution. The template effect of chitosan was proofed by the significantly increased reaction rate. Kinetic studies suggest a pick-up mechanism for this template polymerization. The gelation time of the system can be tuned by chitosan and/or HQ concentration and by temperature. Preliminary electrochemical test suggests that the resultant hydrogel are redox-active. The CV chart of the hydrogel is similar to that of the PHQ polymer synthesized by a sophisticated organometallic polycondensation process. As the synthesis is quite simple, PHQ is an interesting redox polymer and chitosan is attractive biopolymer, the new redox hydrogel is expected to find applications in biomedical areas.

■ ASSOCIATED CONTENT

S Supporting Information. GPC traces of the chitosan sample, NMR spectra and GPC traces of purified PHQ. This material is available free of charge via the Internet at <http://pubs.acs.org>.

■ AUTHOR INFORMATION

Corresponding Author

*E-mail: yongjunzhang@nankai.edu.cn (Y.Z.) and yingguan@nankai.edu.cn (Y.G.).

■ ACKNOWLEDGMENT

Y.G. expresses thanks for financial support from National Natural Science Foundation of China (Grant No. 20974049). Y. Z. expresses thanks for financial support for this work from the Ministry of Science and Technology of China (Grant No. 2007DFA50760) and the National Natural Science Foundation of China (Grant Nos. 20774049 and 20974050).

■ REFERENCES

- (1) Heller, A. *Curr. Opin. Chem. Biol.* **2006**, *10*, 664–672.
- (2) Mano, N.; Yoo, J. E.; Tarver, J.; Loo, Y. L.; Heller, A. *J. Am. Chem. Soc.* **2007**, *129*, 7006–7007.
- (3) Merchant, S. A.; Tran, T. O.; Meredith, M. T.; Cline, T. C.; Glatzhofer, D. T.; Schmidtke, D. W. *Langmuir* **2009**, *25*, 7736–7742.
- (4) Mano, N.; Mao, F.; Heller, A. *ChemBiochem* **2004**, *5*, 1703–1705.
- (5) Mano, N.; Heller, A. *J. Am. Chem. Soc.* **2005**, *127*, 11574–11575.
- (6) Tamaki, T.; Ito, T.; Yamaguchi, T. *J. Phys. Chem. B* **2007**, *111*, 10312–10319.
- (7) Boztas, A. O.; Guiseppi-Elie, A. *Biomacromolecules* **2009**, *10*, 2135–2143.
- (8) Liu, H. M.; Liu, C. X.; Jiang, L. Y.; Liu, J.; Yang, Q. D.; Guo, Z. H.; Cai, X. X. *Electroanalysis* **2008**, *20*, 170–177.
- (9) Brahim, S.; Guiseppi-Elie, A. *Electroanalysis* **2005**, *17*, 556–570.
- (10) Wang, P.; Martin, B. D.; Parida, S.; Rethwisch, D. G.; Dordick, J. S. *J. Am. Chem. Soc.* **1995**, *117*, 12885–12886.
- (11) Cataldo, F. *Polym. Int.* **1998**, *46*, 263–268.

- (12) Furlani, A.; Russo, M. V.; Cataldo, F. *Synth. Met.* **1989**, *29*, 507–510.
- (13) Kimihisa Yamamoto, T. A. H. *Bull. Chem. Soc. Jpn.* **1990**, *63*, 1211–1216.
- (14) Yamamoto, T.; Kimura, T. *Macromolecules* **1998**, *31*, 2683–2685.
- (15) Wang, P.; Amarasinghe, S.; Leddy, J.; Arnold, M.; Dordick, J. S. *Polymer* **1998**, *39*, 123–127.
- (16) MacLaughlin, F. C.; Mumper, R. J.; Wang, J. J.; Tagliaferri, J. M.; Gill, I.; Hinchcliffe, M.; Rolland, A. P. *J. Controlled Release* **1998**, *56*, 259–272.
- (17) Thanou, M. M.; Kotze, A. F.; Scharringhausen, T.; Luessen, H. L.; de Boer, A. G.; Verhoef, J. C.; Junginger, H. E. *J. Controlled Release* **2000**, *64*, 15–25.
- (18) Thanou, M.; Florea, B. I.; Geldof, M.; Junginger, H. E.; Borchard, G. *Biomaterials* **2002**, *23*, 153–159.
- (19) Gobin, A. S.; Froude, V. E.; Mathur, A. B. *J. Biomed. Mater. Res. A* **2005**, *74A*, 465–473.
- (20) Zhao, Z. M.; He, M.; Yin, L. C.; Bao, J. M.; Shi, L. L.; Wang, B. Q.; Tang, C.; Yin, C. H. *Biomacromolecules* **2009**, *10*, 565–572.
- (21) Ong, S. Y.; Wu, J.; Moochhala, S. M.; Tan, M. H.; Lu, J. *Biomaterials* **2008**, *29*, 4323–4332.
- (22) Ishihara, M.; Nakanishi, K.; Ono, K.; Sato, M.; Kikuchi, M.; Saito, Y.; Yura, H.; Matsui, T.; Hattori, H.; Uenoyama, M.; Kurita, A. *Biomaterials* **2002**, *23*, 833–840.
- (23) Allan, G. G.; Peyron, M. *Carbohydr. Res.* **1995**, *277*, 257–272.
- (24) Sadykh-Zade, S. I.; Ragimov, A. V.; Suleimanova, S. S.; LiogonKii, B. I. *Vysokomol. Soedin., Ser. A* **1972**, *14*, 1248–1255.
- (25) Berlin, A. A.; Ragimov, A. V.; Sadykh-Zade, S. I.; Gadzhieva, T. A.; Takhmazov, B. M. *Vysokomol. Soedin., Ser. A* **1975**, *17*, 111–117.
- (26) Ragimov, A. V.; Mamedov, B. A.; LiogonKii, B. I. *Vysokomolekulyarnye Soedineniya, Seriya A* **1977**, *19*, 2538–2542.
- (27) Qin, C. Q.; Dua, Y. M.; Xiao, L. *Polym. Degrad. Stab.* **2002**, *76*, 211–218.
- (28) Guibal, E.; Vincent, T.; Touraud, E.; Colombo, S.; Ferguson, A. *J. Appl. Polym. Sci.* **2006**, *100*, 3034–3043.
- (29) Polowinski, S. *Prog. Polym. Sci.* **2002**, *27*, 537–577.
- (30) Usha, R.; Ramasami, T. *J. Appl. Polym. Sci.* **2002**, *84*, 975–982.
- (31) Maiti, M.; Bhowmick, A. K. *Polym. Eng. Sci.* **2007**, *47*, 1777–1787.
- (32) Richardson, P. H.; Clark, A. H.; Russell, A. L.; Aymard, P.; Norton, I. T. *Macromolecules* **1999**, *32*, 1519–1527.